JOURNAL OF VIROLOGY, Feb. 1997, p. 1097–1106 Vol. 71, No. 2
0022-538X/97/$04.00+0

Phenotypic and Genetic Analysis of *Lymantria dispar* Nucleopolyhedrovirus Few Polyhedra Mutants: Mutations in the *25K FP* Gene May Be Caused by DNA Replication Errors

DAVID S. BISCHOFF AND JAMES M. SLAVICEK*

Forestry Sciences Laboratory, Northeastern Forest Experimental Station, USDA Forest Service, Delaware, Ohio 43015

Received 26 July 1996/Accepted 15 October 1996

We previously demonstrated that polyhedron formation (PF) mutants arise at a high frequency during serial passage of the *Lymantria dispar* nucleopolyhedrovirus (Ld*M*NPV) in the *L. dispar* 652Y cell line (J. M. Slavicek, N. Hayes-Plazolles, and M. E. Kelly, Biol. Control 5:251–261, 1995). Most of these PF mutants exhibited the traits of few polyhedra (FP) mutants; however, no large DNA insertions or deletions that correlated with the appearance of the FP phenotype were found. In this study, we have characterized several of the PF mutants at the phenotypic and genetic levels. Genetic techniques were used to group the mutations in the Ld*M*NPV PF mutants to the same or closely linked genes. Wild-type viruses were recovered after coinfection of *L. dispar* 652Y cells with certain combinations of PF mutants. These viruses were analyzed by restriction endonuclease analysis and found to be chimeras of the original PF mutants used in the coinfections. Marker rescue experiments localized the mutations in one group of PF isolates to the region containing the Ld*M*NPV *25K FP* gene. The mutations in these PF mutants were identified. Four of five of the Ld*M*NPV FP mutants contain small insertions or deletions within the *25K FP* gene. The fifth Ld*M*NPV FP mutant analyzed contained a large deletion that truncated the C terminus of the *25K FP* gene product. All of the deletions occurred within the same potential hairpin loop structure, which had the lowest free energy value (most stable hairpin) of the five potential hairpin loop structures present in the *25K FP* gene. One of the insertion mutants contained an extra base within a repetitive sequence. These types of mutations are likely caused by errors that occur during DNA replication. The relationship between the types of mutations found within the Ld*M*NPV *25K FP* gene and DNA replication-based mutagenesis is discussed.

Nucleopolyhedroviruses (NPVs) are members of the *Baculoviridae* which infect insects and other arthropods. All baculoviruses have a unique infection cycle in that they produce two infectious morphological forms: a budded virus (BV) form and a viral form that is occluded into a protein structure termed a polyhedron. Larvae are infected upon ingestion of the polyhedra and release of the viral particles in the alkaline environment of the midgut. The BV form is produced early during infection, buds from the plasmid membrane, and infects other cell types within the organism. Late during infection the occluded form is generated. Upon death, the larva disintegrates, and the polyhedra are released, thus completing the infection cycle (9). The polyhedron protects the viral particles from environmental elements and is the viral form that is used for biological control of agricultural and forest insect pests.

During replication of NPVs in cell culture, a class of viruses termed few polyhedra (FP) mutants arises at a high frequency. The FP mutant phenotype is characterized by a decrease in polyhedron formation and an increased release of BV. The polyhedra that are produced are noninfectious, as they are virtually devoid of viral particles (16, 18, 26, 32). During serial passage of virus in vitro, FP mutants quickly become the predominant virus type as a consequence of increased BV release (18, 23, 26, 32).

Several FP mutants of *Autographa californica M*NPV (Ac*M*NPV) and *Galleria mellonella M*NPV (Gm*M*NPV) have been characterized. The generation of FP mutants of these viruses has been correlated with the absence of a 25-kDa protein (19) and with the presence of large insertions and deletions (0.4 to 2.8 kbp) within a specific region (36 to 37 map units [m.u.]) of the Ac*M*NPV and Gm*M*NPV viral genomes (13, 19, 23). This region contains the *25K FP* gene, which is essential for polyhedron formation and virion occlusion (2, 3). Several different mutations in the Ac*M*NPV *25K FP* gene were found to generate all phenotypic characteristics of FP mutants (22).

Mutants of *Lymantria dispar M*NPV (Ld*M*NPV) with altered polyhedron formation (PF) phenotypes are generated at a high frequency during serial passage in cell culture (32). Most of these mutants exhibit all of the characteristics of FP mutants. Analysis of genomic restriction endonuclease digestion profiles of 40 of these mutants did not reveal large DNA insertions or deletions that could be correlated with the FP phenotype (32). Recently, we identified and characterized the Ld*M*NPV *25K FP* gene while mapping the mutations in one of the FP mutants, A21-2 (6). This report extends the characterization of a group of Ld*M*NPV PF mutants that exhibit an FP mutant phenotype. The mutations in these viral isolates were mapped to the Ld*M*NPV *25K FP* gene. The majority of the Ld*M*NPV FP mutants analyzed did not contain large insertions or deletions as is commonly found for the Ac*M*NPV and Gm*M*NPV FP mutants.

MATERIALS AND METHODS

Cells and virus. *L. dispar* 652Y cells were grown as monolayers in Goodwin's IPL-52B medium supplemented with 6.25 mM glutamine and 10% fetal bovine serum. Viral isolates were plaque purified as described previously (32). Cell cultures were inoculated with Ld*M*NPV isolate A21-MPV, which produces wild-type polyhedra (33); with wild-type isolate 122(b), 163(b), or B21(a); or with PF mutant A21-2, B21-1, 163-2, 5-6, or 122-2 (32).

* Corresponding author. Mailing address: USDA Forest Service, Northeastern Forest Experimental Station, Forestry Sciences Laboratory, 359 Main Rd., Delaware, OH 43015. Phone: (614) 368-0033. Fax: (614) 368-0152.

Calculation of polyhedron production and BV titers. T25 flasks were seeded with 10^6 cells per flask. The cells were allowed to attach for 1 h before addition of the virus at 10 50% tissue culture infectious dose ($TCID_{50}$) units per cell. The virus was removed after a 1-h adsorption period, and the cells were covered with fresh medium. Polyhedra and BV were recovered at 7 days postinfection (p.i.) after incubation of the cells at 27°C. Polyhedra were isolated, purified, and quantitated as previously described (32).

Polyhedra were prepared and sectioned for transmission electron microscopy as described previously (34). The number of viral nucleocapsids present within polyhedral cross sections was quantitated by counting and expressed as the number of virions present per square micrometer of cross-sectional area per polyhedral cross section.

Viral titers were determined by the endpoint dilution assay first described by Reed and Muench (27) and adapted by Summers and Smith (37). P96 wells were seeded with 10^4 cells per well, and the cells were allowed to attach for 1 h and infected with virus diluted from 10^{-1} to 10^{-11}. The plates were scored after 2 weeks of incubation at 27°C, and the viral titer was expressed as $TCID_{50}$ units per milliliter of cell culture medium.

Coinfection studies. *L. dispar* 652Y cells were seeded into T25 flasks (10^6 cells per flask) and allowed to attach for 1 h. The cells were infected with two of the Ld*M*NPV isolates simultaneously, each at 10 $TCID_{50}$ units per cell. The virus was removed after 1 h, and the cells were covered with fresh medium and incubated at 27°C for 7 days. The BV was plaque purified, and between 96 and 186 plaques from each of the coinfections were used to infect *L. dispar* 652Y cells in P96 plates. After 1 week at 27°C, the infections were scored as exhibiting either an FP or a many polyhedra (MP) phenotype based on the number of polyhedra present. The infection phenotype was termed FP if the majority of the cells contained five or fewer polyhedra and MP if the cells appeared opaque as a consequence of a large number of polyhedra being present. Polyhedron production by several of the MP viral lines was determined as described above.

Viral DNA isolation and Southern blot analysis. BV from plaque-purified Ld*M*NPV isolates was isolated from infected *L. dispar* 652Y cells as described previously (5) and used as a source of genomic DNA for restriction analysis, Southern blot analysis, and marker rescue experiments. Viral DNA was digested with restriction endonucleases and fractionated on 1.0% agarose–Tris-borate-EDTA gels. Southern blot analysis was performed on nitrocellulose with a 1.8-kbp *Sst*II fragment (which contains the *25K FP* gene) labelled with a nick translation kit (Bethesda Research Laboratories) and [α-^{32}P]dCTP (NEN).

Marker rescue mapping of the mutations in the PF mutants. The construction of the Ld*M*NPV A21-MPV cosmid library and the transfection method used in the mapping of the mutations in the PF mutants have been described previously (6). Transfections were carried out with 2.5 μg of mutant viral DNA and 2.5 μg of plasmid DNA with the Lipofectin reagent (Bethesda Research Laboratories).

PCR amplification and sequencing. The *25K FP* alleles were amplified from the viral genome by PCR. Reaction mixtures (100 μl) contained buffer (50 mM KCl, 10 mM Tris-HCl [pH 9.0], 0.1% Triton X-100), 2.0 mM $MgCl_2$, 200 μM deoxynucleotides, 0.5 μM primers, 0.2 μg of viral DNA, and 2.25 U of *Taq* DNA polymerase. Thermal cycling was carried out in a Perkin-Elmer Cetus thermocycler. After denaturation at 94°C for 3 min, 35 cycles were performed at 94°C for 1 min, 48°C for 1 min, and 70°C for 1 min. Primers were designed from the wild-type *25K FP* gene sequence from isolate A21-MPV (5′ primer, GAGCAC ATGACCGTTTCG; 3′ primer, GGTAAATCGAGCACGCTC) (6). After amplification, the entire reaction was run out on a 1% agarose–Tris-borate-EDTA gel, the fragment was excised, and the DNA was purified by using the GeneClean II kit (Bio 101). The fragments were cloned into the TA cloning vector (Invitrogen) or directly sequenced with the Sequenase version 2.0 DNA sequencing kit (U.S. Biochemicals) by using protocols supplied with the kits. α-^{35}S-dATP was supplied by NEN. Sequence analysis was done with the MacVector program (International Biotechnologies, Inc.). Hairpin loop structures were first identified with the HAIRPIN program and then further analyzed with the RNAFOLD program, both from PCGENE (IntelliGenetics, Inc.).

RNA isolation and Northern blot analysis. Ld*M*NPV-infected *L. dispar* 652Y cells were harvested at 48 h p.i. Cytoplasmic RNA was isolated as described by Friesen and Miller (20). Total RNA was separated on 1.2% agarose gels containing formaldehyde and transferred to nitrocellulose. Northern blot analysis was performed as described by Mahmoudi and Lin (24). A 30-base oligonucleotide (GACTCTCGCTCACGTTGCGGTCGATTTCGG) which hybridizes within the *25K FP* coding region (6) was end labelled with [γ-^{32}P]ATP (NEN) and used as a strand-specific probe to detect the *25K FP* transcripts. The transcripts were analyzed with a Bio-Rad model 620 video densitometer.

In vitro transcription and translation of the *25K FP* alleles. The 934-bp PCR-amplified *25K FP* alleles were cloned into the TA cloning vector (Invitrogen). The genes were expressed from these constructs with the T_NT coupled reticulocyte lysate system and T7 RNA polymerase (Promega) according to the directions provided with the kit. The expressed protein was labelled by the addition of [^{35}S]methionine (NEN). Reaction products were analyzed by sodium dodecyl sulfate-polyacrylamide gel electrophoresis and autoradiography.

Nucleotide sequence accession numbers. The nucleotide sequence accession numbers of the sequences contained in this paper are U79640 to U79644.

RESULTS

Characteristics of the PF mutants. Ld*M*NPV isolates A21-2, B21-2, 122-2, 163-2, and 5-6 were previously identified in a study on FP mutant formation (32, 34). Each of the plaque-purified isolates was characterized in terms of polyhedron production, $TCID_{50}$, and relative polyhedral virion density. Analysis of the polyhedra produced by the mutants by electron microscopy revealed that they were normal in terms of shape and size, although they were virtually devoid of viral nucleocapsids (Fig. 1). The mutants produced significantly fewer (analysis of variance [ANOVA] with Fisher's PLSD, $P < 0.05$) polyhedra than an isolate that produces wild-type polyhedra, A21-MPV (Fig. 2A). The nucleocapsid density of A21-MPV polyhedra is approximately 10-fold greater (ANOVA with Fisher's PLSD, $P < 0.05$) than polyhedra produced by the mutants (Fig. 2B). The amount of BV released by the mutants is also significantly altered. All of the mutant isolates released significantly more (ANOVA with Fisher protected least significant difference, $P < 0.05$) BV than did A21-MPV (Fig. 2C). Comparison of the number of polyhedra produced, the relative polyhedral nucleocapsid density, and the amount of BV released by each of the mutants indicated that they were not significantly different from each other (ANOVA with Fisher's PLSD, $P < 0.05$).

Genetic analysis of Ld*M*NPV PF mutants. A genetic approach was initially used to determine if the mutations responsible for the FP phenotypes of isolates A21-2, B21-1, 122-2, 163-2, and 5-6 were in the same or closely linked genes. Another PF mutant, PFM-C, which produces large cuboidal polyhedra that lack viral nucleocapsids, was used in this investigation, since it contained a mutation that maps to a region distinct from the *25K FP* gene. This mutation has been mapped to the *polyhedrin* gene region (4.0 to 6.5 m.u.) through marker rescue studies (7). An Ac*M*NPV mutant, isolate M5, with a similar phenotype has been previously described (10). The mutation in the M5 isolate was localized and found to be within the *polyhedrin* gene (11, 12).

L. dispar 652Y cells were coinfected with all combinations of the putative FP mutants and isolate PFM-C. In all of the coinfections the cells were found to contain few polyhedra at 7 days p.i. (data not shown). BV from the coinfections was plaque purified, and the plaques were used to infect *L. dispar* 652Y cells to determine if wild-type virus was generated through recombination between mutant viruses. Virus exhibiting a wild-type polyhedron synthesis phenotype was found after coinfection of isolates A21-2, B21-2, 122-2, 163-2, and 5-6 with isolate PFM-C (Fig. 3). Wild-type virus was not detected after coinfection of cells with combinations of isolates A21-2, B21-1, 122-2, 163-2, and 5-6 (Fig. 3), nor was it detected in control infections with the Ld*M*NPV PF mutants used in this investigation (data not shown).

Characteristics of the recombinant viruses. MP viral lines from coinfections of isolate PFM-C with isolates A21-2, B21-1, 122-2, 163-2, and 5-6 were plaque purified and characterized in terms of the number of polyhedra produced per flask. These MP viruses produced wild-type levels of polyhedra (ranging from approximately 5×10^7 to 1×10^8 polyhedra per flask) and produced significantly more polyhedra (ANOVA with Fisher's PLSD, $P < 0.05$) than the original PF isolates used in the study (data not shown). There was no significant difference (ANOVA with Fisher's PLSD) in the amounts of polyhedra produced by the MP isolates and isolate A21-MPV.

Some of the MP viruses generated by the coinfections were analyzed by restriction endonuclease analysis to determine if they were chimeric viruses formed through recombination be-

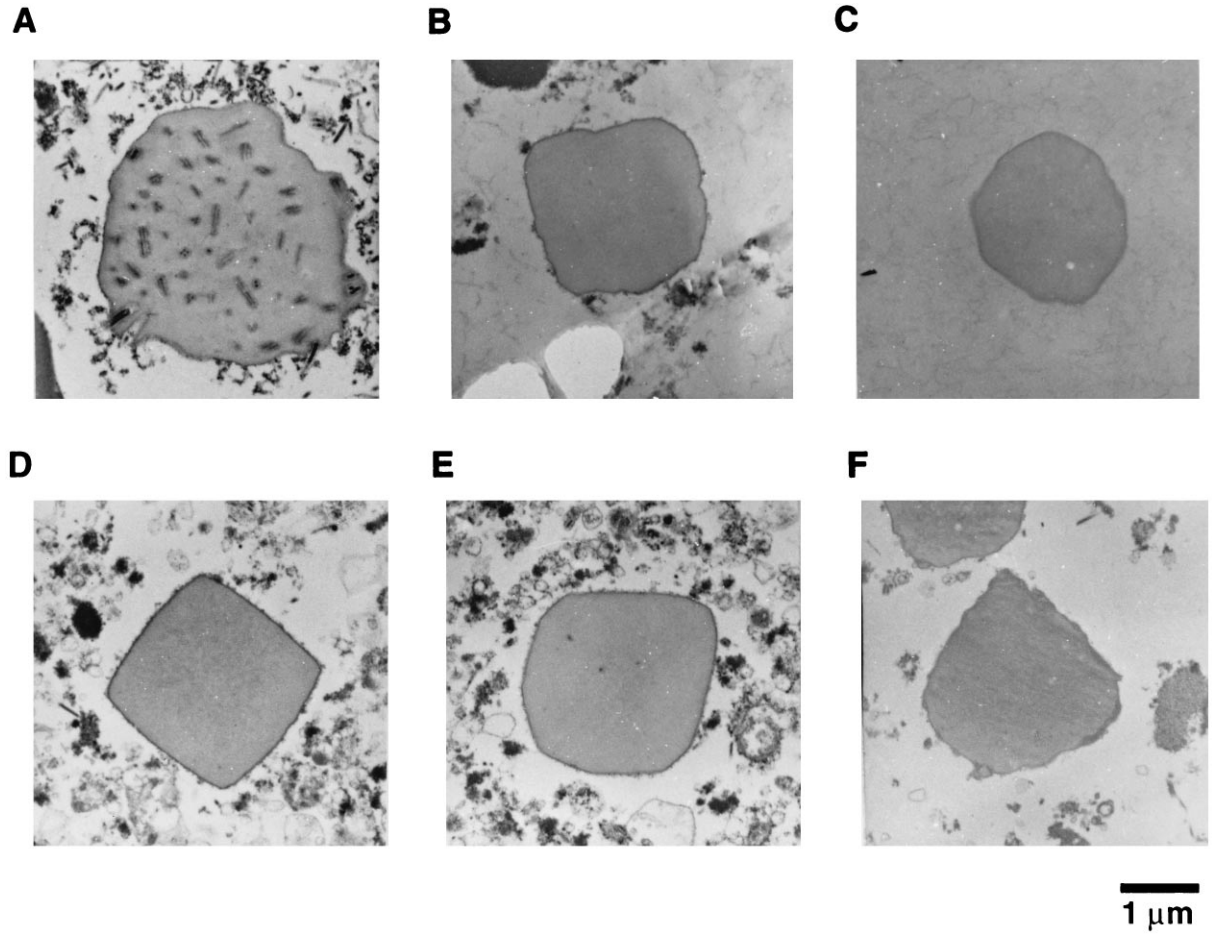

FIG. 1. Electron micrographs of polyhedral cross sections of A21-MPV, which produces wild-type polyhedra (A), and of the PF mutants A21-2 (B), B21-1 (C), 122-2 (D), 163-2 (E), and 5-6 (F).

tween the two viral strains used in the coinfection. The original Ld*M*NPV viral strains [B21(a), 122(b), and 163(b)] used for a study on FP mutant formation (32) are genotypic variants (data not shown). Isolates A21-2 and PFM-C have identical restriction endonuclease digestion patterns, and therefore, MP viruses generated in that coinfection could not be analyzed in this manner. The genomic restriction digestion profiles of three MP viruses were analyzed and found to contain fragments that originated from each of the mutants used in the coinfection (data not shown). For example, the MP isolate PFM-C × 163-2-A11-B5 was found to contain a 3.5-kbp fragment from isolate 163-2 that is close to the *polyhedrin* gene and a 6.2-kbp fragment from isolate PFM-C that is proximal to the *25K FP* gene. The proximity of these fragments to the *polyhedrin* and *25K FP* genes suggests that these genes originated from isolates 163-2 and PFM-C, respectively, thereby generating a virus with the MP phenotype.

Marker rescue of the mutations in the FP isolates. The mutation within the A21-2 isolate had previously been mapped to the 4.3-kbp *Bam*HI/*Eco*RI fragment between 39.8 and 42.5 m.u. on the viral genome (6). This region had been further subcloned, and the A21-2 mutation was localized to a 1.8-kbp *Sst*II fragment and then to a 934-bp fragment (40.3 to 40.8 m.u.) containing only the wild-type *25K FP* allele from A21-MPV (Fig. 4A) (6). Marker rescue experiments conducted with three of the other four isolates (B21-1, 5-6, and 122-2) that were genetically grouped with the A21-2 mutation (see coinfection data) showed that the wild-type phenotype (dark, opaque cells with many polyhedra [Fig. 4C]) could also be restored to these mutants with this 934-bp fragment. This result, in conjunction with the phenotype of isolates B21-1, 5-6, and 122-2, suggests that the FP phenotype of these mutants is due to mutations in the *25K FP* gene.

Genomic analysis of Ld*M*NPV isolate 163-2. All of the Ld*M*NPV FP mutants analyzed in detail to date exhibit *Bgl*II genomic restriction endonuclease patterns that are identical to those of their respective wild-type viral lines (32). However, attempts to generate a 934-bp fragment containing the *25K FP* gene in isolate 163-2 through PCR amplification with primers that were 5′ and 3′ to the *25K FP* gene were unsuccessful (data not shown). To further investigate the *25K FP* gene region in isolate 163-2, *Bam*HI/*Eco*RI genomic digestion profiles were generated and compared to the digestion profiles of isolates A21-MPV and 163(b) (data not shown). Isolate 163-2 was missing the 5.2- and 4.3-kbp fragments that were present upon *Bam*HI/*Eco*RI restriction of both A21-MPV and 163(b) (data not shown). In addition, 163-2 contained a 8.2-kbp fragment not present in the other two isolates. After *Eco*RI restriction, this same 8.2-kbp fragment was present in 163-2 and was absent in 163(b). When this gel was probed with the 4.3-kbp *Bam*HI/*Eco*RI fragment (39.8 to 42.5 m.u.), which contains the *25K FP* gene, the 4.3-kbp fragment hybridized in A21-MPV

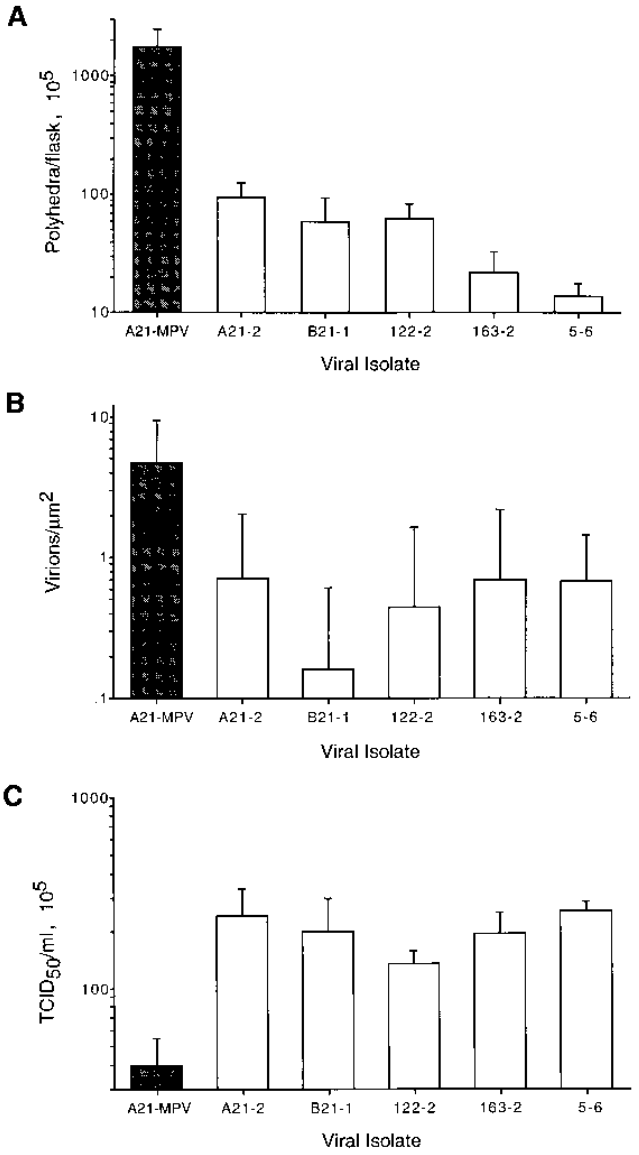

FIG. 2. Polyhedron production characteristics of A21-MPV, which produces wild-type polyhedra, and the PF mutants. (A) Number of polyhedra produced per flask at 7 days p.i. The values are the averages and standard deviations for three determinations. (B) Virion density within polyhedral cross sections expressed as the number of virions per square micrometer of cross-sectional surface area. Values are the averages and standard deviations for at least 25 cross sections. (C) BV production expressed as $TCID_{50}$ units per milliliter of cell culture medium. Values are the averages and standard deviations for three determinations.

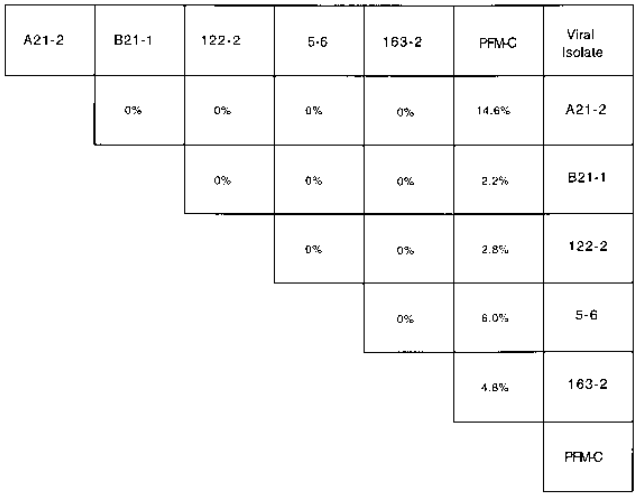

FIG. 3. Percentages of plaques from coinfections of PF mutants that exhibit an MP phenotype.

and 163(b) as expected, but the new 8.2-kbp fragment hybridized in 163-2 (*Bam*HI/*Eco*RI restriction). When restricted with *Eco*RI, the same 8.2-kbp fragment hybridized in 163-2, and the expected 9.5-kbp *Eco*RI fragment hybridized in both A21-MPV and 163(b) (data not shown). These results indicate that 163-2 contains a 1.3-kbp deletion within the *25K FP* region of the genome which also deletes the *Bam*HI site located at 39.8 m.u. on the viral genome (Fig. 4A).

Analysis of the mutations in the FP mutants. In order to characterize the putative mutations in the *25K FP* genes in isolates A21-2, B21-1, 122-2, and 5-6, the *25K FP* alleles were PCR amplified and sequenced. Oligonucleotide primers were used to amplify the 934-bp fragment containing the *25K FP* gene (Fig. 4A). Because the allele could not be amplified from 163-2 due to the large deletion, the 8.2-kbp *Eco*RI fragment was cloned, and the sequence of this region was determined.

Two of the isolates (A21-2 and 5-6) contained single-base-pair insertions within the *25K FP* coding region (Fig. 5A). A21-2 contained an extra cytosine residue after residue 191 (numbering beginning with the ATG start codon (6), and 5-6 contained an extra thymidine residue within a string of thymidine residues between positions 207 and 214 (the exact site of the insertion cannot be determined). The two insertions are within 16 to 24 bp of each other and approximately 200 bp downstream (with respect to the direction of transcription) of the ATG start codon. The other three mutants (122-2, B21-2, and 163-2) contained deletions within the *25K FP* coding sequence. 122-2 and B21-2 contained small deletions: a 24-bp deletion in 122-2 (positions 316 to 339) and an 8-bp deletion in B21-2 (positions 305 to 312). One endpoint of the 1.3-kbp deletion in 163-2 begins at position 314. These three deletions are approximately 115 bp downstream (with respect to the direction of transcription) of the insertions in isolates A21-2 and 5-6.

The expected effects of the mutations on the proteins expressed in these mutants are shown in Fig. 5B. Isolate 122-2 should produce a nearly wild-type protein with an 8-amino-acid (aa) in-frame deletion (aa 106 to 113) internal to the protein. Isolates B21-2, A21-2, 5-6, and 163-2 are expected to produce frameshifted proteins with N termini identical to that of wild-type 25K FP protein and unique C termini. B21-2 would produce a 173-aa protein (versus 217 aa for the wild type) with a fusion after aa 101. Isolate 163-2 should produce a 127-aa fusion protein after residue 105. The additional 23 aa after the fusion point in isolate 163-2 are from sequences that are approximately 1.3-kbp downstream of the *25K FP* gene. A21-2 and 5-6 should both produce 176-aa proteins, with fusions after residues 63 and 69, respectively.

In vitro transcription and translation of *25K FP* alleles. The PCR-amplified alleles were cloned into the TA cloning vector (Invitrogen) under control of the T7 promoter. These constructs were used to express the mutant proteins in a rabbit reticulocyte in vitro transcription and translation system. The proteins were separated by sodium dodecyl sulfate-polyacryl-

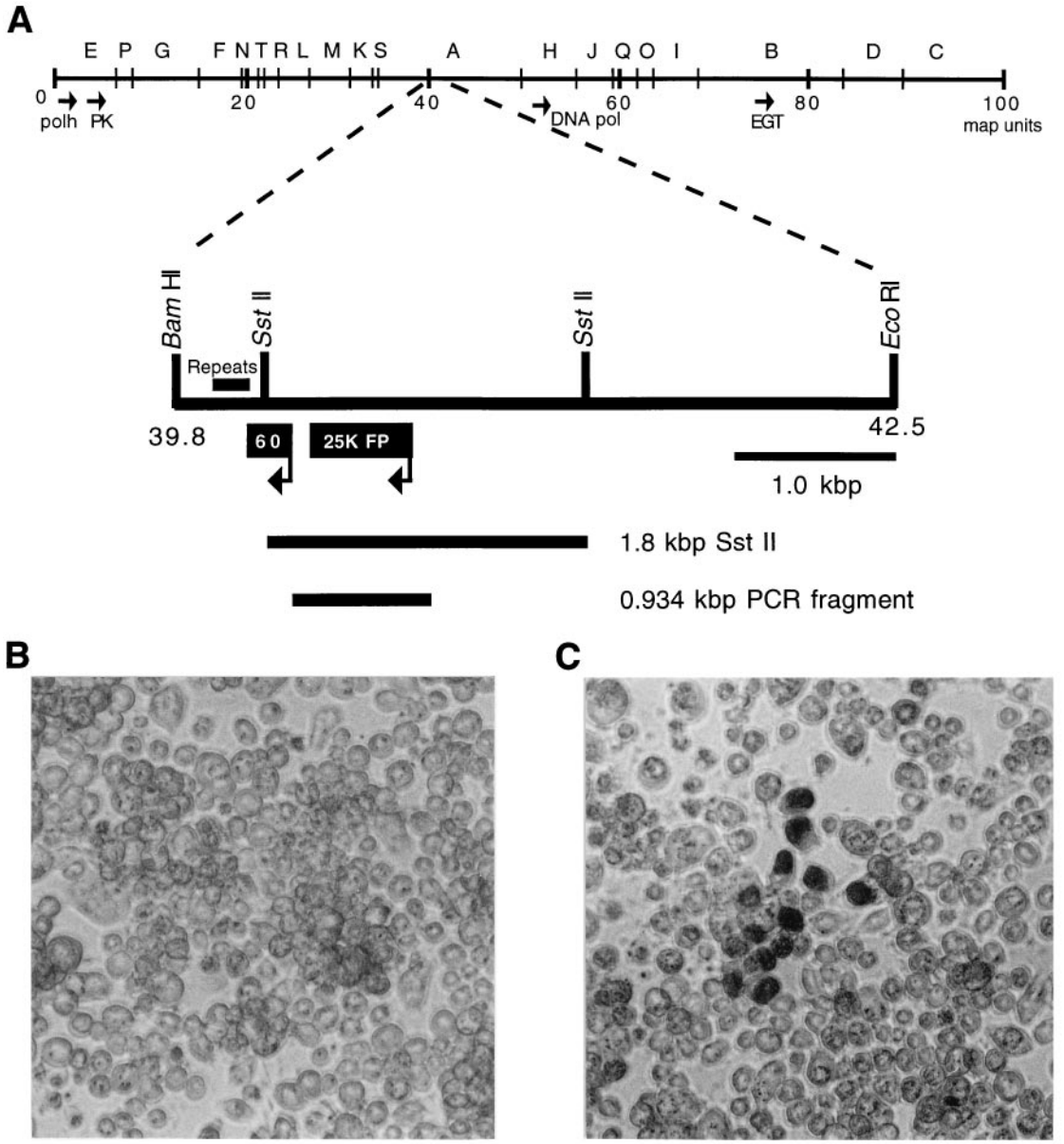

FIG. 4. Marker rescue mapping of the PF mutations. (A) *Bgl*II restriction map showing the location of the 4.3-kbp *Bam*HI/*Eco*RI fragment (39.8 to 42.5 m.u. on the viral genome) and subclones which could repair the PF mutations. The *Bgl*II fragments are indicated by the letters. The locations of other Ld*M*NPV genes are indicated, as follows: polh, *polyhedrin* (35); EGT, *ecdysteriod UDP-glucosyltransferase* (28), DNA pol, *DNA polymerase* (8); and PK, *viral protein kinase* (5). (B and C) Appearance of *L. dispar* 652Y cells visualized under light microscopy after cotransfection with 2.5 μg of 122-2 viral DNA alone (B) or together with 2.5 μg of a plasmid, pDB152, containing the 0.934-kbp PCR fragment with the wild-type *25K FP* gene from A21-MPV (C). Cells were visualized with a Nikon Diaphot-TMD inverted microscope and photographed at ×100 magnification.

amide gel electrophoresis and visualized by autoradiography. Wild-type (A21-MPV) 25K FP protein runs as a doublet with an apparent molecular mass of 27 kDa (data not shown) (6). The doublet may be due to translational initiation at a methionine residue that is internal to the *25K FP* coding sequence (6). The other alleles all produced proteins (doublets) with sizes similar to those expected from the DNA sequences (data not shown). Isolate 122-2 produced 25-kDa proteins (23 kDa expected), whereas B21-1 produced 19-kDa proteins (18 kDa expected). Both A21-2 and 5-6 produced proteins of 20 kDa (19 kDa expected).

Transcriptional analysis of *25K FP* mutant genes. The transcriptional patterns of the *25K FP* RNAs in the FP isolates and the MP viruses from which they were derived were analyzed. A 30-base oligonucleotide was designed from the nucleotide sequence and used as a strand-specific probe to determine the transcription patterns of the *25K FP* genes (6).

The *25K FP* gene is expressed in the MP viruses [A21-MPV, 122(b), B21(a), 163(b)] as two late transcripts (0.95 and 1.3 kb) at high levels (Fig. 6A) and as a 2.5-kb transcript at lower levels (Fig. 6B). The transcription patterns of most of the mutant isolates (A21-2, 5-6, 122-2, and B21-2) contain all three of the transcripts, although the relative levels of transcription of these transcripts differ from that of each of the wild-type viruses. The transcripts for A21-MPV, A21-2, 122(b), 122-2, B21(a), and B21-1 were digitized and standardized to the expression of the

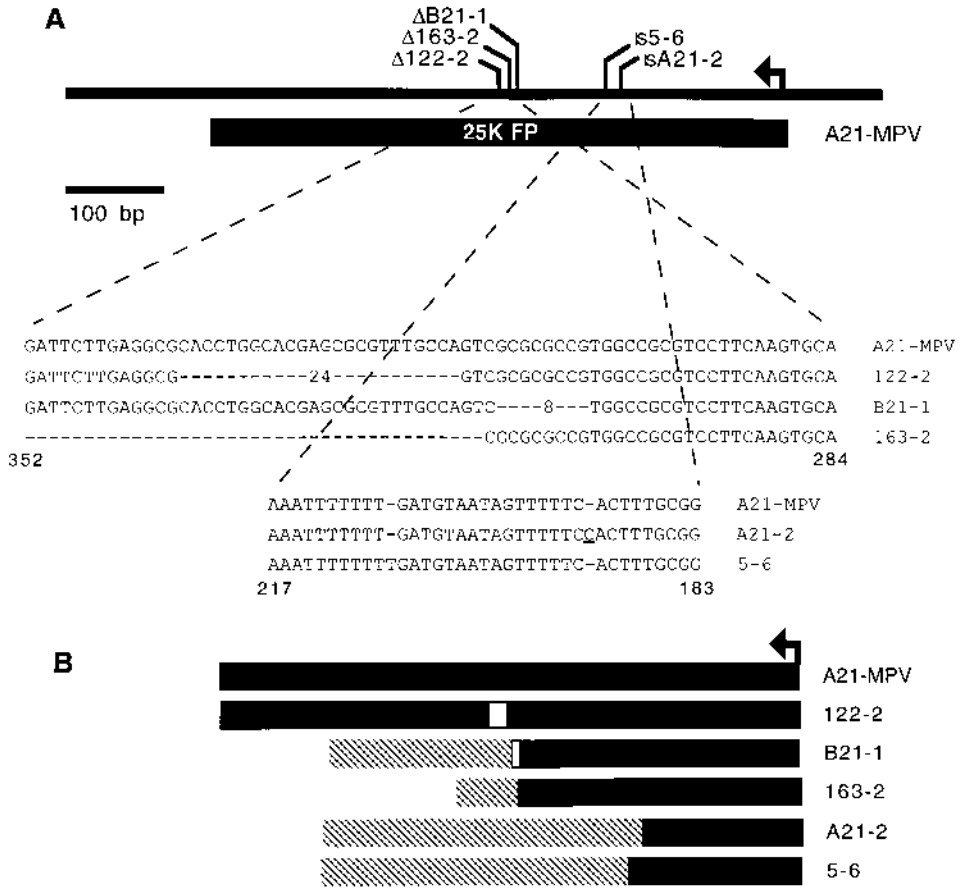

FIG. 5. Sequence analysis of the *25K FP* genes in the FP mutants. (A) Schematic presentation of the locations and sequences of the *25K FP* mutations within the Ld*M*NPV FP mutants. The sequences are numbered with respect to the ATG start codon of the wild-type *25K FP* gene. Dashes indicated the positions of the deletions or insertions (IS) in the FP mutants. The inserted base in A21-2 is underlined. (B) Predicted effects of the mutations on the 25K FP proteins expressed in the FP mutants. Solid areas, regions homologous to the wild-type protein; open areas, deleted regions; hatched areas, nonhomologous regions within the fusion proteins as a consequence of the frameshift mutations.

0.95-kb transcripts in each lane. Isolate 5-6 was not analyzed in this manner since there is no corresponding wild-type isolate that was purified prior to the passage in which 5-6 was isolated. In all three cases, there was a slight decrease in the transcription level of the 1.3-kb transcript and an increase in the level of the 2.5-kb transcript for each of the FP mutants relative to the respective wild-type viral lines (Table 1). Of the five mutants, only isolate 163-2 has a drastically altered transcription pattern, with a 1.4-kb transcript that is expressed at high levels (Fig. 6) instead of the 0.95- or 1.3-kb transcript seen in the wild-type isolates.

DISCUSSION

All of the PF mutants analyzed in this study exhibited the same phenotype of reduced polyhedron formation and virion occlusion and increased BV release. These traits are the same as those exhibited by the Ac*M*NPV, Gm*M*NPV, and Ld*M*NPV FP mutants (16, 18, 22, 26, 32). A genetic approach was used to group these five PF mutants (Fig. 3). The coinfection results suggested that the mutations in these isolates were in the same locus, which was distinct from that mutated in the PFM-C mutant. The validity of this approach was confirmed with marker rescue experiments that indicated that the genes mutated in the five mutants were in similar locations on the viral genome and over 59 kbp from the PFM-C mutation. Since the FP phenotype in the Ac*M*NPV and Gm*M*NPV mutants is the result of inactivation of the *25K FP* gene (3, 22) and since the A21-2 mutation had already been mapped to the region on the genome (40.3 to 40.8 m.u.) that contains the *25K FP* gene (6), it was very likely that all of these PF isolates contained mutations within the *25K FP* gene.

Further marker rescue experiments and sequence analysis of the *25K FP* alleles within the PF mutants confirmed that these isolates contained mutations within this gene. Four of the five isolates (A21-2, 5-6, B21-1, and 122-2) contained small insertions (1 bp) or deletions (8 and 24 bp). Only one isolate (163-2) contained a large deletion (1.3 kbp deleted). This is in contrast to the case for the Ac*M*NPV and Gm*M*NPV FP mutants characterized to date, which frequently contain large insertions or deletions within the *25K FP* gene, but in agreement with earlier work on the Ld*M*NPV FP mutants (32, 33) which indicated that the isolates all have *Bgl*II restriction patterns that are identical to the patterns of the parental wild-type viruses. This finding suggested either that Ld*M*NPV FP mutants may arise through a mechanism different than that for the formation of FP mutants in Ac*M*NPV and Gm*M*NPV or that they may arise through a similar mechanism but are not readily detectable by restriction analysis. FP mutants with restriction patterns identical to those of wild-type viruses have also been isolated for Ac*M*NPV and Gm*M*NPV, although the exact mutations re-

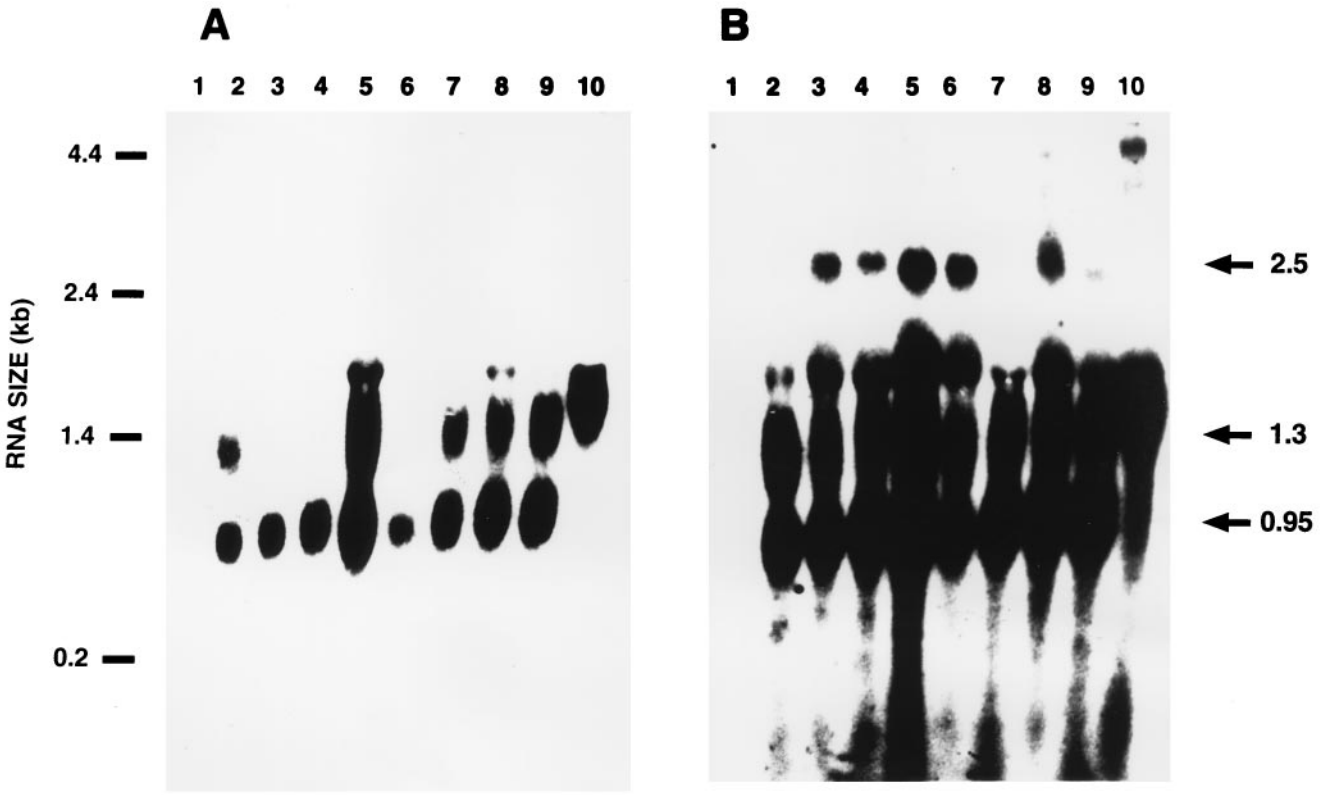

FIG. 6. Expression analysis of the LdMNPV *25K FP* transcripts within each of the FP isolates. *L. dispar* 652Y cells were infected with 10 $TCID_{50}$ units of the LdMNPV isolates per cell. At 48 h p.i. the cells were harvested, and cytoplasmic RNA was isolated. Total RNA (40 μg) was separated by formaldehyde-agarose gel electrophoresis, blotted, and probed with a *25K FP* strand-specific, ^{32}P-labelled oligonucleotide. Lanes: 1, uninfected cells; 2, A21-MPV; 3, A21-2; 4, 5-6; 5, 122(b); 6, 122-2; 7, B21(a); 8, B21-1; 9, 163(b); 10, 163-2. Different exposures of the same Northern blot are shown in panels A and B. RNA size standards are indicated on the left, and the sizes of the transcripts are indicated on the right.

sponsible for the FP phenotype in these isolates have not been characterized (13).

All five of the LdMNPV mutants exhibited the same FP phenotype. This was also observed by Harrison and Summers (22), who reported that all of the AcMNPV mutations which had any part of the *25K FP* gene deleted had a similar effect on polyhedron synthesis and virion occlusion. The AcMNPV mutants analyzed by Harrison and Summers (22) included mutants with an N-terminal deletion (first 25 aa deleted), a C-terminal deletion (last 90 aa deleted), and a nearly complete deletion (only the first 20 aa remaining), suggesting that all parts of the protein are required for function. Four of five of the LdMNPV mutants are expected to produce C-terminally truncated proteins with at least the first 63 aa in common with the wild-type protein. Of these mutants, three of four have been expressed in vitro and produce proteins of the expected sizes. Since the *25K FP* gene region could not be PCR amplified from isolate 163-2 due to the deletion, this allele was not characterized in vitro.

TABLE 1. Relative levels of expression of the *25K FP* transcripts

Isolate[a]	Relative level of expression[b]		
	0.95-kb transcript	1.3-kb transcript	2.5-kb transcript
A21-MPV	1.00	1.11	0.15
A21-2	1.00	0.82	0.24
122(b)	1.00	0.95	0.29
122-2	1.00	0.92	0.58
B21(a)	1.00	0.84	0.03
B21-1	1.00	0.81	0.28

[a] A21-MPV, 122(b), and B21(a) produce wild-type polyhedra; A21-2, 122-2, and B21-1 are FP isolates.
[b] Standardized to the level for the 0.95-kb transcript for each isolate.

The 122-2 25K FP protein is of interest since it produces a nearly wild-type protein (with an 8-aa in-frame deletion) yet the deletion is sufficient to give the FP mutant attributes of decreased polyhedron formation and virion occlusion and increased BV release. Alignment of the LdMNPV and AcMNPV 25K FP proteins revealed that over these 8 aa the two proteins exhibit 50% amino acid identity, although these residues are within one of the less homologous regions of the proteins (exhibiting only 40% amino acid identity in this region [6]). The 122-2 protein was expressed in vitro and produces a protein doublet of the expected size; however, the protein's stability in vivo has not been determined. Therefore, it is possible either that these residues are required directly for the 25K FP protein to function properly or that the deletion of these residues may indirectly affect the function by altering the secondary structure and/or stability of the protein in vivo. No noticeable overall reduction in the levels of isolate 122-2 *25K FP* gene transcripts was observed in comparison to those for the 122(b) wild-type virus, suggesting that the FP phenotype in 122-2 is

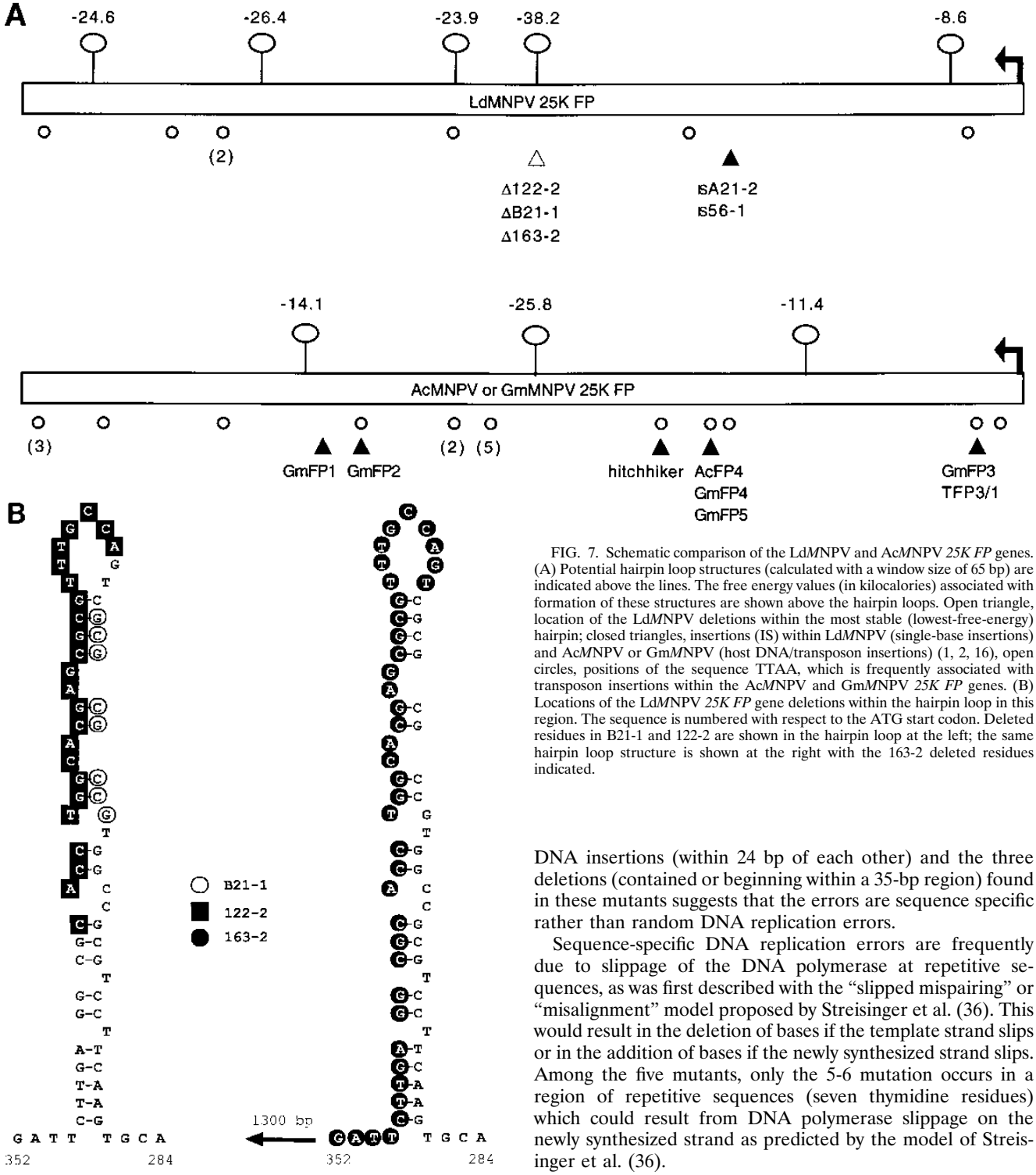

FIG. 7. Schematic comparison of the Ld*M*NPV and Ac*M*NPV *25K FP* genes. (A) Potential hairpin loop structures (calculated with a window size of 65 bp) are indicated above the lines. The free energy values (in kilocalories) associated with formation of these structures are shown above the hairpin loops. Open triangle, location of the Ld*M*NPV deletions within the most stable (lowest-free-energy) hairpin; closed triangles, insertions (IS) within Ld*M*NPV (single-base insertions) and Ac*M*NPV or Gm*M*NPV (host DNA/transposon insertions) (1, 2, 16), open circles, positions of the sequence TTAA, which is frequently associated with transposon insertions within the Ac*M*NPV and Gm*M*NPV *25K FP* genes. (B) Locations of the Ld*M*NPV *25K FP* gene deletions within the hairpin loop in this region. The sequence is numbered with respect to the ATG start codon. Deleted residues in B21-1 and 122-2 are shown in the hairpin loop at the left; the same hairpin loop structure is shown at the right with the 163-2 deleted residues indicated.

not likely to be due to decreased transcription or mRNA instability.

The small insertions and deletions that have been identified in the Ld*M*NPV *25K FP* gene may suggest that this gene has a high frequency of DNA replication-based mutagenesis rather than transposon-based mutagenesis as is seen in the Ac*M*NPV and Gm*M*NPV FP mutants. The close proximity of the two DNA insertions (within 24 bp of each other) and the three deletions (contained or beginning within a 35-bp region) found in these mutants suggests that the errors are sequence specific rather than random DNA replication errors.

Sequence-specific DNA replication errors are frequently due to slippage of the DNA polymerase at repetitive sequences, as was first described with the "slipped mispairing" or "misalignment" model proposed by Streisinger et al. (36). This would result in the deletion of bases if the template strand slips or in the addition of bases if the newly synthesized strand slips. Among the five mutants, only the 5-6 mutation occurs in a region of repetitive sequences (seven thymidine residues) which could result from DNA polymerase slippage on the newly synthesized strand as predicted by the model of Streisinger et al. (36).

DNA replication errors also occur at regions containing palindromic sequences that may result in the formation of hairpin loops or cruciform structures (14, 30, 31). At these structures the DNA polymerase pauses, which interferes with DNA replication and may promote slippage of the nascent DNA, resulting in mutagenesis through a DNA synthesis error mechanism. Pausing of the RNA polymerase at a hairpin loop may also activate DNA repair pathways (after repeated attempts at transcription), triggering gratuitous and potentially

error-prone repair even though no DNA damage is present (15, 21, 39).

Sequence analysis of the LdMNPV *25K FP* region reveals five potential hairpin loop structures that could form within the *25K FP* gene, with structure energies ranging from −8.6 to −38.2 kcal (Fig. 7A). The endpoints of the three deletions in isolates B21-1, 122-2, and 163-2 are all within the most stable (lowest-free-energy) hairpin loop structure (−38.2 kcal [calculated by using a window size of 65 bp]) (Fig. 7B), which is in close proximity to a second hairpin loop structure (−23.9 kcal). Computer analysis with a larger window (160 bp) reveals that this region has the potential to form a structure containing both loops with a energy of −81.2 kcal (data not shown). In contrast, analysis of the AcMNPV *25K FP* gene (3) reveals three potential hairpin loop structures, with the most stable one having a free energy of −25.8 kcal (Fig. 7A). Alignment of the DNA sequences of the LdMNPV and the AcMNPV genes reveals that the most stable hairpin loops are in the same location in each of these genes (Fig. 7A). Additional analysis is necessary to determine if the AcMNPV and GmMNPV FP mutants which have DNA restriction patterns identical to those of the wild-type viruses also contain deletions within this hairpin loop structure. Since the LdMNPV *25K FP* gene is transcribed starting at 48 h p.i. and after DNA replication has been initiated (20 h p.i.) (29), it is likely that the mutations would be due to the pausing of the DNA polymerase (DNA synthesis error mechanism) rather than due to stalling of the RNA polymerase (gratuitous-repair mechanism).

Several of the AcMNPV and GmMNPV FP mutants contained host DNA insertions within the *25K FP* gene which resulted in the direct duplication of a 4-nucleotide target sequence, TTAA (Fig. 7A) (4, 17, 25). Sequence analysis of the *25K FP* genes from LdMNPV and AcMNPV reveals the presence of this target sequence 18 times in AcMNPV but only 7 times in LdMNPV (Fig. 7A). The finding that a higher proportion of AcMNPV and GmMNPV FP mutants than of LdMNPV FP mutants contain insertions could be due to the greater number of TTAA target sites within the AcMNPV and GmMNPV *25K FP* genes. Alternatively, the higher proportion of transposon insertions in AcMNPV and GmMNPV FP mutants might be due to a higher rate of transposition in AcMNPV- or GmMNPV-infected cells than in LdMNPV-infected cells. It is tempting to speculate as to whether this increased rate of transposition is a property of the different cell lines used or of the virus itself.

The majority of the work that has been done to investigate the role of DNA replication, hairpin loop formation, and cruciform formation in mutagenesis has been done by using *Escherichia coli* as a model system, in which the bacterium acquires drug resistance as a consequence of deletion of the hairpin loop structure (30, 38, 40). The ability to do site-directed mutagenesis of the hairpin within the *25K FP* gene coupled with the quick formation of FP mutants in LdMNPV may provide a unique system to investigate the effect of hairpin loop structures on DNA replication-based mutagenesis in eukaryotes.

ACKNOWLEDGMENTS

We are grateful for the technical assistance of Melissa J. Mercer with characterization of the FP and recombinant MP viruses and of Mary Ellen Kelly with the transmission electron microscopy. We also thank M. J. Fraser and Suzanne M. Thiem for critical review of the manuscript.

This research was supported by funds from the American Cyanamid Company and the U.S. Department of Agriculture, Forest Service, Northeastern Forest Experiment Station.

REFERENCES

1. **Bauser, C. A., T. A. Elick, and M. J. Fraser.** 1996. Characterization of *hitchhiker*, a transposon insertion frequently associated with baculovirus FP mutants derived upon passage in the TN-368 cell line. Virology **216:**235–237.
2. **Beames, B., and M. D. Summers.** 1988. Comparison of host cell DNA insertions and altered transcription at the site of insertions in few polyhedra baculovirus mutants. Virology **162:**206–220.
3. **Beames, B., and M. D. Summers.** 1989. Location and nucleotide sequence of the 25K protein missing from baculovirus few polyhedra (FP) mutants. Virology **168:**344–353.
4. **Beames, B., and M. D. Summers.** 1990. Sequence comparison of cellular and viral copies of host cell DNA insertions found in *Autographa californica* nuclear polyhedrosis virus. Virology **174:**354–363.
5. **Bischoff, D. S., and J. M. Slavicek.** 1994. Identification and characterization of a protein kinase gene in the *Lymantria dispar* multinucleocapsid nuclear polyhedrosis virus. J. Virol. **68:**1728–1736.
6. **Bischoff, D. S., and J. M. Slavicek.** 1996. Characterization of the *Lymantria dispar* nucleopolyhedrovirus *25K FP* gene. J. Gen. Virol. **77:**1913–1923.
7. **Bischoff, D. S., and J. M. Slavicek.** Unpublished data.
8. **Bjornson, R. M., B. Glocker, and G. F. Rohrmann.** 1992. Characterization of the nucleotide sequence of the *Lymantria dispar* nuclear polyhedrosis virus DNA polymerase gene region. J. Gen. Virol. **73:**3177–3183.
9. **Blissard, G. W., and G. F. Rohrmann.** 1990. Baculovirus diversity and molecular biology. Annu. Rev. Entomol. **35:**127–155.
10. **Brown, M., P. Faulkner, M. A. Cochran, and K. L. Chung.** 1980. Characterization of two morphology mutants of *Autographa californica* nuclear polyhedrosis virus with large cuboidal inclusion bodies. J. Gen. Virol. **50:**309–316.
11. **Carstens, E. B.** 1982. Mapping the mutation site of an *Autographa californica* nuclear polyhedron morphology mutant. J. Virol. **43:**809–818.
12. **Carstens, E. B., A. Krebs, and C. E. Gallerneault.** 1986. Identification of an amino acid essential to the normal assembly of *Autographa californica* nuclear polyhedrosis virus polyhedra. J. Virol. **58:**684–688.
13. **Cary, L. C., M. Goebel, B. G. Corsaro, H. H. Wang, E. Rosen, and M. J. Fraser.** 1989. Transposon mutagenesis of baculoviruses: analysis of *Trichoplusia ni* transposon IFP2 insertions within the FP-locus of nuclear polyhedrosis viruses. Virology **172:**156–169.
14. **Darlow, J. M., and D. R. F. Leach.** 1995. The effects of trinucleotide repeats found in human inherited disorders on palindrome inviability in *Escherichia coli* suggest hairpin folding preferences *in vivo*. Genetics **141:**825–832.
15. **Datta, A., and S. Jinks-Robertson.** 1995. Association of increased spontaneous mutation rates with high levels of transcription in yeast. Science **268:** 1616–1619.
16. **Fraser, M. J.** 1987. FP mutation of nuclear polyhedrosis viruses: a novel system for the study of transposon-mediated mutagenesis, p. 265–293. *In* K. Maramorosch (ed.), Biotechnology in invertebrate pathology and cell culture. Academic Press, San Diego, Calif.
17. **Fraser, M. J., J. S. Brusca, G. E. Smith, and M. D. Summers.** 1985. Transposon-mediated mutagenesis of a baculovirus. Virology **145:**356–361.
18. **Fraser, M. J., and W. F. Hink.** 1982. The isolation and characterization of the MP and FP plaque variants of *Galleria mellonella* polyhedrosis virus. Virology **117:**366–378.
19. **Fraser, M. J., G. E. Smith, and M. D. Summers.** 1983. Acquisition of host cell DNA sequences by baculoviruses: relationship between host DNA insertions and FP mutants of *Autographa californica* and *Galleria mellonella* nuclear polyhedrosis viruses. J. Virol. **47:**287–300.
20. **Friesen, P. D., and L. K. Miller.** 1985. Temporal regulation of baculovirus RNA: overlapping early and late transcripts. J. Virol. **54:**394–400.
21. **Hanawalt, P. C.** 1994. Transcription-coupled repair and human disease. Science **266:**1957–1958.
22. **Harrison, R. L., and M. D. Summers.** 1995. Mutations in the *Autographa californica* multinucleocapsid nuclear polyhedrosis virus 25 kDa protein gene result in reduced virion occlusion, altered intranuclear envelopment and enhanced virus production. J. Gen. Virol. **76:**1451–1459.
23. **Kumar, S., and L. K. Miller.** 1987. Effects of serial passage of *Autographa californica* nuclear polyhedrosis virus in cell culture. Virus Res. **7:**335–349.
24. **Mahmoudi, M., and V. K. Lin.** 1989. Comparison of two different hybridization systems in Northern transfer analysis. BioTechniques **7:**331–333.
25. **Miller, D. W., and L. K. Miller.** 1982. A virus mutant with an insertion of a *copia*-like transposable element. Nature (London) **299:**562–564.
26. **Potter, K. N., P. Faulkner, and W. F. Hink.** 1976. Strain selection during serial passage of *Trichoplusia ni* nuclear polyhedrosis virus. J. Virol. **18:**1040–1050.
27. **Reed, L. J., and H. Muench.** 1938. A simple method of estimating fifty percent endpoints. Am. J. Hyg. **27:**493–497.
28. **Riegel, C. I., C. Lanner-Herrera, and J. M. Slavicek.** 1994. Identification and characterization of the ecdysteroid UDP-glucosyltransferase gene of the *Lymantria dispar* multinucleocapsid nuclear polyhedrosis virus. J. Gen. Virol. **75:**829–838.
29. **Riegel, C. I., and J. M. Slavicek.** Unpublished data.
30. **Rosche, W. A., T. Q. Trinh, and R. R. Sinden.** 1995. Differential DNA secondary structure-mediated deletion mutation in the leading and lagging

strands. J. Bacteriol. **177:**4385–4391.
31. **Sinden, R. R., G. Zheng, R. G. Brankamp, and K. N. Allen.** 1991. On the deletion of inverted repeated DNA in *Escherichia coli*: effects of length, thermal stability, and cruciform formation *in vivo*. Genetics **129:**991–1005.
32. **Slavicek, J. M., N. Hayes-Plazolles, and M. E. Kelly.** 1995. Rapid formation of few polyhedra mutants of the *Lymantria dispar* multinucleocapsid nuclear polyhedrosis virus during serial passage in cell culture. Biol. Control **5:**251–261.
33. **Slavicek, J. M., M. J. Mercer, M. E. Kelly, and N. Hayes-Plazolles.** 1996. Isolation of a baculovirus variant that exhibits enhanced polyhedra production stability during serial passage in cell culture. J. Invert. Pathol. **67:**153–160.
34. **Slavicek, J. M., J. Podgwaite, and C. Lanner-Herrera.** 1992. Properties of two *Lymantria dispar* nuclear polyhedrosis virus isolates from the microbial pesticide Gypchek. J. Invert. Pathol. **59:**142–148.
35. **Smith, I. R. L., N. A. M. van Beek, J. D. Podgwaite, and H. A. Wood.** 1988. Physical map and polyhedrin gene sequence of the *Lymantria dispar* nuclear polyhedrosis virus. Gene **71:**97–105.
36. **Streisinger, G., Y. Okada, J. Emrich, J. Newton, A. Tsugata, E. Terzaghi, and M. Inouye.** 1966. Frameshift mutations and the genetic code. Cold Spring Harb. Symp. Quant. Biol. **31:**77–84.
37. **Summers, M. D., and G. E. Smith.** 1987. A manual of methods for baculovirus vectors and insect cell culture procedures. Texas Agricultural Experiment Station Bulletin no. 1555.
38. **Trinh, T. Q., and R. R. Sinden.** 1993. The influence of primary and secondary DNA structure in deletion and duplication between direct repeats in *Escherichia coli*. Genetics **134:**409–422.
39. **Wang, G., M. M. Seidman, and P. M. Glazer.** 1996. Mutagenesis in mammalian cells induced by triple helix formation and transcription-coupled repair. Science **271:**802–805.
40. **Weston-Hafer, K., and D. E. Berg.** 1991. Deletions in plasmid pBR322: replication slippage involving leading and lagging strands. Genetics **127:**649–655.